Proceedings of 25th Conference
on Decision and Control
Athens, Greece • December 1986

SHAPE CONTROL IN SENDZIMIR MILLS USING BOTH CROWN AND INTERMEDIATE ROLL ACTUATORS

J. V. Ringwood

School of Electronic Engineering,
National Institute for Higher Education,
Glasnevin, Dublin 9, Ireland.

M. J. Grimble

Industrial Control Unit,
Dept. of Electronic and Electrical Engineering,
University of Strathclyde, Glasgow G1 1XW, U.K.

ACKNOWLEDGEMENT

The authors are grateful for the support of GEC Electrical Projects, Rugby and the British Steel Corporation, Sheffield. We are grateful for the contributions to the project by Mr. A. Kidd of GEC and Mr. A. Bill of BSC. Thanks are also due to Dr. K. Dutton of Sheffield City Polytechnic and Dr. M.A. Johnson and Dr. J.F. Barrett of the Industrial Control Unit, University of Strathclyde for their many helpful comments.

ABSTRACT

The solution to the shape control problem for a Sendzimir mill, utilising the As-U-Roll shape actuators, is well understood. The tapered first intermediate rolls, however, provide a more powerful shape control device. This paper describes a control philosophy utilising both the As-U-Rolls and first intermediate rolls as shape control mechanisms. A robustness result for the design is developed, which is useful, since such a mill is normally used to roll a large number of materials, and a single controller must therefore be employed for many different schedules. Finally, a variety of simulation results are presented, showing the transient responses and performance of the multivariable shape control system.

1. INTRODUCTION

The shape control problem (the control of internal strip stress) in Sendzimir mills, utilising the As-U-Roll (AUR) actuators, has been studied in some depth [1], [2] and indeed a shape control scheme, previously described [3], utilising the AUR's is now approaching the final commissioning stages. Automatic shape control by means of the first intermediate rolls (FIR's) as a shape control device has, to date, received relatively little attention. Fig.1 shows the location of both sets of actuators on the Sendzimir mill. The first intermediate rolls may be moved in or out of the rolling cluster, and since they possess a taper (see Fig.2), they can affect the roll bending profile in the mill and hence the shape profile [4]. Their primary function is to control shape at the strip edges, and it is the edge zones of the strip which are covered by the tapered part of the rolls. Due to their proximity to the strip, the FIR's provide a very powerful shape control device, and can produce high order bending in the workrolls. This is in contrast to the As-U-Rolls, whose bending effects are smoothed out by the stiffness of the intervening second intermediate and back-up rolls (see Fig.1). The relative importance of the FIR's as a shape control device is increased when consideration is given to the mechanical restrictions which inhibit certain profiles being set up on the AUR's. These limitations arise due to the danger of fracturing the back-up roll shaft by demanding extreme (and opposite) displacements in adjacent actuators. A certain amount of safety tolerance is achieved by limiting the AUR actuator profiles to fourth order (through parameterisation [1]), but an analysis by Dutton [3] has shown this to be insufficient. The FIR's, on the other hand, do not suffer from such relative positional restrictions (within their range of movement).

2. THE SENDZIMIR MILL MODEL

The Sendzimir mill model has been adequately described elsewhere [3][5][6] and merely the form of the final (linearised) transfer function model is given here as:

$$y_m = g(s)[G_a \;\; G_i]\, u_m \qquad (1)$$

where

y_m = measured shape profile (ϵR^8)
u_m = actuator inputs (ϵR^{10})

G_a ($\epsilon R^{8\times 8}$) and G_i ($\epsilon R^{8\times 2}$) are matrices of linearised constant gains, relating roll-gap shape profile to actuator inputs (for AUR's and FIR's respectively) The scalar transfer function g(s) has the form:

$$g(s) = \frac{e^{-\tau_1 s}}{(1 + 2.0s)(1 + \tau_2 s)(1 + \tau_3 s)} \qquad (2)$$

where $\tau_1 = D/v$, $\tau_2 = D_1/v$

D = dist. from roll-gap to shapemeter(2.91m)
D_1 = distance from roll-gap to coiler (5.32m)
v = strip velocity in metres/second

τ_3 corresponds to a shapemeter time constant, varied for the different strip speeds as:

speed (m/s)	0 -> 2	2 -> 5	5 -> 15
τ_0 (secs)	1.43	0.74	0.3

3. SHAPE PROFILE PARAMETERISATION

Though the shapemeter output is modelled as an 8-point profile, the actual shapemeter produces a number of outputs ranging from 17 to 31, depending on strip width. In order to provide a consistant number of outputs, a shape profile parameterisation is used. Instead of controlling the actual shape or stress pattern, a number of parameters, or attributes, of the shape profile are controlled. Following a least squares analysis based on a number of equally-spaced available measurements [3], [5], the best parameter fit is given by the Gram polynomials [7]. The first four Gram polynomials (excluding the zeroth order) are roughly

linear, quadratic, cubic and quartic in form. Shape profiles corresponding to the higher order polynomials are not required to be controlled and more importantly, attempts to set up high-order roll bending in the mill can cause cracking of the back-up rolls. For this reason, a transformation is also used to limit the number of control inputs to the AUR actuators. This transformation is similar to that for the outputs, but in this case four control inputs are used to control eight actuators (hence limiting the bending to fourth order) . A transformation matrix, corresponding to eight available measurements, evaluated from the Fisher and Yeates tables [8] is:

$$\begin{bmatrix} -0.54 & -0.38 & -0.23 & -0.08 & 0.08 & 0.23 & 0.38 & 0.54 \\ 0.54 & 0.08 & -0.23 & -0.38 & -0.38 & -0.23 & 0.08 & 0.54 \\ -0.43 & 0.31 & 0.43 & 0.18 & -0.18 & -0.43 & -0.31 & 0.43 \\ 0.28 & -0.53 & -0.12 & 0.36 & 0.36 & -0.12 & -0.53 & 0.28 \end{bmatrix}$$

$$= P \qquad (3)$$

The linearised (and parameterised) mill TFM is given as:

$$G(s) = g(s)\ P[G_a P^T \quad PG_i] \qquad (4)$$

4. A MULTILEVEL CONTROL SOLUTION

In this approach, the FIR's are used to control different shape parameters than the AUR's, and a cross-coupling term is used to alleviate interaction problems. The multilevel control structure is shown in Fig.3.

4.1 Design approach

In this approach, two parameters are controlled by each actuator set. It is not important at this stage how the parameters are allocated, the prime consideration being that the FIR and AUR parameterisations are mutually orthogonal. The Gram polynomials, mentioned in Section 3, are used for shape profile parameterisation. The matrices P_1 and P_2 will be used to represent the AUR and FIR parameterisations respectively, where P_1, $P_2 \in R^{2\times 8}$. The reasoning behind the multilevel structure is relatively straightforward. Since the FIR system has only two inputs, it can, at most, control only two shape parameters. The FIR loop, therefore, is chosen as the independent loop, and is diagonalised with respect to the parameter set P_2, in the arrangement shown in Fig.3, using $K_i \in R^{2\times 2}$.
However, some undesireable shape components in the range space of P_1 are produced at the roll-gap by the FIR's, since they have no control over this parameter set. From knowledge of G_i, these components may be evaluated, and the parameter demand in the AUR loop adjusted accordingly via the cross-coupling term, $K_{ia} \in R^{2\times 2}$.
The AUR loop (dependent loop) can, unlike the FIR's, control all four parameters, since it has eight inputs (reduced to four by the parameterisation). For the current configuration, however, only two parameters (corresponding to P_2) are required to be controlled. The demand in the parameters corresponding to P_2 are set to zero, therefore ensuring that no undesireable shape components in the range space of P_2 are produced at the roll-gap by the AUR's. The AUR controller, $K_a \in R^{8\times 4}$ (shown in Fig.12), as a result, has four inputs, two of which are zero. An expression for the equivalent 2-input/8-output controller, $K_a \in R^{8\times 2}$ (shown in Fig.4) may be obtained [5] as:

$$K_a = (Q_1 - Q_2 Q_4^{-1} Q_3)^{-1} + (Q_2 - Q_1 Q_3 - 1 Q_4)^{-1} \qquad (5)$$

where $Q_1 = P_1 G_a P^T$, $Q_2 = P_1 G_a P^T$
$Q_3 = P_2 G_a P^T$, $Q_4 = P_2 G_a P^T$

Theorem
The system is diagonalised by the choise of controllers K_i, K_a' and K_{ia} as follows:

$$K_i = (P_2 G_i)^{-1} \qquad (6)$$
$$K_a' = (P G_a P^T)^{-1} \qquad (7)$$
where $$P = \begin{bmatrix} P_1 \\ P_2 \end{bmatrix} \qquad (8)$$
$$K_{ia} = P_1 G_i (P_2 G_i)^{-1} \qquad (9)$$

Proof
Ignoring the plant dynamics (since the dynamics in each path are identical), the system forward path transfer function matrix may be written (from Fig.3) as:

$$F = \begin{bmatrix} P_1 \\ P_2 \end{bmatrix} [G_a P^T \quad G_i] \begin{bmatrix} K_a & -K_a K_{ia} \\ 0 & K_i \end{bmatrix}$$

$$= \begin{bmatrix} P_1 G_a P^T K_a & P_1 G_i K_i - P_1 G_a P^T K_a K_{ia} \\ P_2 G_a P^T K_a & P_2 G_i K_i - P_2 G_a P^T K_a K_{ia} \end{bmatrix} \qquad (10)$$

where $F \in R^{4\times 4}$

For the system to be diagonal, it is required that:

$$F = I_4$$

Equivalently, if F is partitioned as:

$$F = \begin{bmatrix} F_1 & F_2 \\ F_3 & F_4 \end{bmatrix} \qquad (11)$$

with obvious identification of F_1, F_2, F_3, and $F_4 \in R^{2\times 2}$, then the required conditions on F_1, F_2, F_3 and F_4 are:

$$F_1 = F_4 = I_2 \quad , \quad F_2 = F_3 = 0 \qquad (12)$$

Examining each term in turn:
(i) For block F_1: Using (5):

$$F_1 = Q_1 (Q_1 - Q_2 Q_4^{-1} Q_3)^{-1} + Q_2 (Q_2 - Q_1 Q_3^{-1} Q_4)^{-1} \qquad (13)$$

Applying the Householder inversion formula [10] to the term $(Q_1 - Q_2 Q_4^{-1} Q_3)^{-1}$ yields:

$$(Q_1 - Q_2 Q_4^{-1} Q_3)^{-1} = Q_1^{-1} + Q_1^{-1} Q_2 (Q_4 - Q_3 Q_1^{-1} Q_2)^{-1} Q_3 Q_1^{-1}$$
$$= Q_1^{-1} - Q_1^{-1} Q_2 (Q_2 - Q_1 Q_3^{-1} Q_4)^{-1} \qquad (14)$$

substituting back for $(Q_1 - Q_2 Q_4^{-1} Q_3)^{-1}$ in (13) gives:

$$F_1 = Q_1 [Q_1^{-1} - Q_1^{-1} Q_2 (Q_2 - Q_1 Q_3^{-1} Q_4)^{-1}] + Q_2 (Q_2 - Q_1 Q_3^{-1} Q_4)^{-1}$$
$$= I_2 - Q_2 (Q_2 - Q_1 Q_3^{-1} Q_4)^{-1} + Q_2 (Q_2 - Q_1 Q_3^{-1} Q_4)^{-1}$$
$$= I_2 \qquad (15)$$

(ii) For block F_3:

$$F_3 = Q_3 (Q_1 - Q_2 Q_4^{-1} Q_3)^{-1} + Q_4 (Q_2 - Q_1 Q_3^{-1} Q_4)^{-1}$$
$$= (Q_1 Q_3^{-1} - Q_2 Q_4^{-1})^{-1} + (Q_2 Q_4^{-1} - Q_1 Q_3^{-1})^{-1}$$
$$= 0 \qquad (16)$$

(iii) For block F_2:

$$F_2 = P_1 G_i K_i - P_1 G_a P^T K_a K_{ia} \qquad (17)$$

It has already been shown in (15) that $P_1 G_a P^T K_a = I_2$, giving:

$$F_2 = P_1G_iK_i - K_{ia} \quad (18)$$

Using (6) and (9) yields:

$$F_2 = P_1G_i(P_2G_i)^{-1} - P_1G_i(P_2G_i)^{-1} = 0 \quad (19)$$

(iv) For block F_4:

$$F_4 = P_2G_iK_i - P_2G_aP^TK_aK_{ia} \quad (20)$$

Using equation (16) and (10) gives:

$$F_4 = P_2G_iK_i = P_2G_i(P_2G_i)^{-1} = I_2 \quad (21)$$

and it may be concluded that the system shown in Fig.3 is diagonal for the controller choices of (6) to (9). The overall controller matrix is:

$$C1 = \begin{bmatrix} K_a' & -K_a'K_{ia} \\ 0 & K_i \end{bmatrix} \quad (22)$$

The system has therefore been reduced to four identical SISO systems in parallel, each with forward path transfer function g(s)k(s), k(s) being chosen to give suitable stability and dynamic performance characteristics.

4.2 Parameter Allocation

A number of combinations of parameters, which are to be controlled by each actuator set, exist. Though 6 ($= {}^4C_2$) combinations are possible, only one case will be examined here, one other case being documented in [5]. Writing P, the transformation matrix given in Section 3, as:

$$P^T = (p_1\ p_2\ p_3\ p_4) \quad ; \quad p_1,p_2,p_3,p_4 \in R^8 \quad (23)$$

the case under consideration may be identified as:

$$P_1{}^T = (p_1\ \ p_2) \quad , \quad P_2{}^T = (p_3\ \ p_4)$$

that is, the AUR's controlling the linear and quadratic shape parameters, and the FIR's controlling the cubic and quartic shape parameters. This choice of P_1 and P_2 accords with rolling practice (manual shape control), where the AUR's are used to control up to (and including) second order shape profiles, the FIR's being used to control shape at the strip edges (high order profiles). The reasoning behind this practice is that by setting up low order profiles on the AUR's, the restrictions regarding their relative movements are not violated, allowing their full potential to be realised. By using the FIR's to control the high order (edge) profiles, their best potential is realised, since their influence is greatest at the strip edges.

5. A UNIFIED DESIGN PHILOSOPHY

It will be shown later that the design presented in Section 4 has poor robustness to variations in the mill gain matrices. The following section presents an alternative diagonalisation procedure with improved robustness properties.

5.1 Design Approach

The closed-loop structure which will be used in this design procedure is shown in Fig.4 The linearised (and transformed) plant transfer function matrix excluding dynamics is given from (4) as:

$$G = P[G_aP^T \quad G_i] \quad (24)$$

noting that $G \in R^{4\times6}$. Let a right inverse, $N \in R^{6\times4}$, be defined such that:

$$[PG_aP^T \quad PG_i]\ N = I_4 \quad (25)$$

Again, the system has been reduced to four SISO systems in parallel, each with forward path transfer function g(s)k(s).

5.2 Choice of a Right Inverse

It can be shown [1] that PG_aP^T ($\in R^{4\times4}$) is full rank and hence that the matrix G (given in (24)) is full row rank. Therefore, a right inverse, N, exists but is not necessaraily unique [10]. The resulting design freedom may be exploited by minimising the norm of the control inputs to the plant. This helps to ensure that actuator wear is kept to a minimum and that the actuators are restricted to their working range. The required right inverse which minimises u^Tu is evaluated as:

$$C2 = G^T(GG^T)^{-1} \quad (26)$$

6. DYNAMIC PRECOMPENSATOR DESIGN

k(s) was designed for low, medium and high speed plants using a combination of frequency response and simulation trials. Fig.6 shows the frequency response for the uncompensated and compensated systems. The controller transfer function (for a single loop) is:

$$k(s) = \frac{k_1\ (1 + 2.0s)}{(1 + 1000s)(1 + 0.9s)} \quad (27)$$

where k_1 is given as:

strip speed (m/s)	0 -> 2	2 -> 5	5 -> 15
k_1	100	200	500

Note that a simple gain scheduling technique is used in k(s) for changes in strip speed. If finer tuning is required, k_1 could be made a continuous function of strip speed. Good steady-state response is ensured by placing a pole at s = 0.001.

7. ROBUSTNESS ANALYSIS

Gauge reduction on the Sendzimir 20-roll Cold Rolling Mill is a multi-pass, multi-schedule process. For each steel coil rolled, a particular schedule is chosen according to strip width, initial gauge, final gauge, quality and material of the coil. The schedule also specifies the number of passes the strip will undergo to achieve the required reduction in gauge. Since the percentage reduction varies with the pass number, and the hardness of the material increases as it is reduced, the mill matrices, G_m and G_i, are a function of pass number. It is not practical to store a precompensator matrix for each schedule and pass, and hence a smaller subset must be used. It is important to have a measure of the allowable variations in the elements of G_m and G_i to see to what extent this simplification may be achieved while maintaining stability. It is also important to know the extent to which the modelling inaccuracies in the mill matrices will be tolerated. For the current problem, an analysis based on element variations in G_m is appropriate. The advantage of using element data is that the information on the system structure is retained in addition to the position and relative magnitudes of the errors. Furthermore, data on the errors in

the elements of G_m is readily obtainable. This type of approach has recently been shown to be a useful and viable route to robust design in general [11],[12].

7.1 Robustness W.R.T. Errors in G_a and G_i

In the following analysis, it is assumed that a precompensator matrix, $K(s) \in R(s)^{6\times4}$, has been designed for a nominal plant, G(s), but that G_a and G_i are subject to perturbations $\Delta_a \in R^{8\times8}$ and $\Delta_i \in R^{8\times2}$ respectively. Note that:

$$K(s) = K\,k(s) \qquad (28)$$

where $K \in R^{6\times4}$ is the diagonalising controller (described in Sections 4 and 5), and k(s) the dynamic precompensator (described in Section 6). It is assumed that k(s) stabilises the plant dynamic transfer function, g(s). Let a transformed perturbation matrix, Δ, be defined as:

$$\Delta = [P\Delta_a P^T,\ P\Delta_i] \qquad (29)$$

The stability of the feedback system is described by the return difference:

$$|I_4 + g(s)k(s)P[(G_a+\Delta_a)P^T,\ (G_i+\Delta_i)]K| =$$

$$|I_4+g(s)k(s)P[G_aP^T,\ G_i]K+g(s)k(s)P[\Delta_aP^T,\ \Delta_i]K|$$

$$= |A||B| \qquad (30)$$

where

$$A = I_4 + g(s)k(s)P[G_aP^T,\ G_i]K$$

$$B=I_4+\{g(s)k(s)P[\Delta_aP^T,\Delta_i]K\}^{-1}g(s)k(s)P[G_aP^T,G_i]K$$

Clearly, system stability is determined by the 'B' determinant, since the 'A' determinant is merely the return difference of the unperturbed system. By noting that:

$$[PG_aP^T \quad PG_i]\,K = I_4 \qquad (31)$$

which is true for both the multilevel and the right-inverse controllers, the stability of the perturbed system is determined by the condition:

$$|I_4 + (1 + gk)^{-1}gk\Delta K| \neq 0 \quad \text{for} \quad Re(s) \geq 0 \qquad (32)$$

substituting from equation (29) and dropping the s-dependence for clarity. The condition in (32) may be replaced by the more conservative condition:

$$1 > \sum_{j=1}^{4} |F_{rj}(s)| \qquad 1 \leq r \leq 4 \qquad (33)$$

where F_{rj} are the elements of the matrix $F(s) \in R(s)^{4\times4}$, given by:

$$F(s) = (1 + gk)^{-1}gk\ \Delta K \qquad (34)$$

Since F(s) is strictly proper and analytic and bounded in the interior of D, the suprema are achieved on the imaginary axis, and the frequency dependent condition of (33) may be replaced by the frequency independent condition:

$$1 > \sum_{j=1}^{4} \sup_{\omega\geq0} |F_{rj}(j\omega)| \qquad 1 \leq r \leq 4 \qquad (35)$$

Defining the maximum value of the closed loop frequency response as:

$$\gamma = \sup_{\omega\geq0} |(1 + gk)^{-1}gk| \qquad (36)$$

the condition expressed in (35) becomes:

$$1 > \sum_{j=1}^{4} |\gamma(\Delta K)_{rj}| \qquad (37)$$

Given the perturbation, Δ, the controller matrix, K, and γ (from a Nicholl's Chart), it is possible to determine the stability of the perturbed system by examining the inequalities given in (54). For the two cases under consideration, the controller matrix, K, becomes:

$$K = C1 \qquad (38)$$

where C1 is given in (22) for the multilevel controller, and

$$K = C2 \qquad (39)$$

where C2 is given in (26) for the right inverse controller.

7.2 Mismatched Controller Evaluation

An example is taken here, whereby a diagonalising controller matrix, K, calculated for Schedule X Pass 1, is to be used with a plant corresponding to Schedule Y Pass 1. It is required to evaluate the inequalities of (37) for this case to determine if stability is retained. No intermediate numerical results are provided but the calculation route is as follows:

(i) Evaluate Δ_a and Δ_i from the mill matrices pertaining to the different schedules.
(ii) Evaluate the transformed perturbation matrix, Δ.
(iii) Calculate γ, the maximum value of the closed loop frequency response from a Nicholl's Plot.
(iv) Evaluate the product ΔK and multiply by γ to give the inequality coefficients.
(v) Sum the resulting coefficients over the rows and test for stability.

The resulting inequalities, calculated for both controllers C1 and C2 are as follows:

Controller C1:	Controller C2:
1 > 0.7114	1 > 0.4499
1 > 0.8932	1 > 0.2612
1 > 0.6601	1 > 0.4078
1 > 0.8547	1 > 0.4073

The above inequalities were evaluated using a value of γ = 0.99 (obtained from a Nicholl's Chart), pertaining to a medium speed plant. Simulation results for this mismatched case are given in Section 8. It is seen that, for the mismatched case under consideration, the inequality set is satisfied, indicating that stability is retained. For some cases, however, it has been shown [5] that though stability is retained (confirmed by simulation tests), the inequaliy set has not been satisfied. This is due to the conservatism built into the analysis via equation (33). In such cases, system stability (or rather instability) must be confirmed by simulation tests. Note, however, that when the inequalities are satisfied, stability is guaranteed.

8. PERFORMANCE EVALUATION

Nonlinear simulation tests were used to assess the performance of the shape control schemes developed in the preceeding sections. was non-time varying, and is shown in Fig.7. The output shape profile variations with time are shown in Figs.6 and 7 for controllers C1 and C2 respectively. The corresponding shape parameter variations (first to fourth order) with time are shown in Figs.8 and 9 for C1 and C2, respectively. Note that control is applied after the simulation has been allowed to run for three seconds. The shape control for both C1 and C2 is good (as seen from Figs.6 and 7), the residual profiles consisting of high-order shape components. This may be validated by checking Figs.8 and 9, where the steady-state error is seen to be

zero for the four shape parameters which are controlled. Figs.10 and 11 show the shape profile and parameter varaitions for a mismatched C1 controller for the case given in Section 7.2. These graphs verify that no instability is present, as predicted by the set of inequalities.

9. DISCUSSION

Two controller designs have been examined, one of which minimises the control inputs to the plant. The consequences of this minimisation will now be examined more fully. This special feature of C2 results in the elements of the C2 matrix being small in magnitude compared to C1. A quantitative measure of the magnitude of the matrix elements is given as the Euclidean norm [13], which is defined as:

$$||K||_E = \left[\sum_{i=1}^{6} \sum_{j=1}^{4} k_{ij}^2 \right]^{1/2} \qquad (40)$$

where k_{ij} are the elements of the given controller matrix. Calculation of the Euclidean norm for C1 and C2 gives:

CONTROLLER	$\|\|K\|\|_E$
C1	0.941
C2	0.183
C3	4.423

Table 9

Note the inclusion of a norm value corresponding to a controller 'C3'. C3 corresponds to a multilevel controller, where the AUR's are used to control second and fourth order shape profiles (even orders) and the FIR's are used to control first and third order profiles (odd orders). This controller is documented fully in [5]. Controller C3 is included in this section to allow a more complete controller comparison to be made. From equation (37), the robustness of a particular controller is seen to depend on the magnitude of the elements of the controller matrix. Some conclusions, therefore, regarding the relative robustness of the various controllers may be made with respect to Table 9. Controller C2 appears to be the most robust, with C1 and C3 being progressively less robust. This is significant, since C1 and C3 both contain zero blocks (see equation (22)), and hence one would expect the matrix norms to be small. If the efficiency of a controller is defined as that which minimises control effort, then some conclusions regarding the efficiency of the different controller structures may also be deduced from Table 9. In controller C2, all four parameters may be set up on both the AUR's and FIR's. The relative distribution of the parameters on each actuator set is determined in an 'optimal' sense so that the control input norms are minimised. In C1 and C3 the parameter allocation is fixed initially and the resulting matrix norms are large. The exceptionally large norm for C3 indicates the difficulty of setting up first and third order profiles on the FIR's and second and fourth order profiles on the AUR's. It may therefore be concluded that this structure is inefficient (validated by simulation results given in [5]).

10. CONCLUSIONS

A variety of designs for the shape control of a Sendzimir mill utilising both AUR and FIR actuators have been developed. The different designs allow different combinations of shape parameters to be set up on the different actuator sets. While the right inverse controller of Section 5 was shown to have the best performance and robustness properties, a multilevel structure may be more appropriate from mechanical or operator considerations (recalling that the configuration of Section 4.2 corresponds with manual rolling practice). The robustness of the control philosophies developed was expressed in terms of a series of strict linear inequalities. These inequalities are easily calculated from the elemental data available via the static model of Gunawardene [6]. Though the stability predictions of the analysis is sometimes conservative, satisfaction of the inequalities guarantees stability.

It is envisaged that a singular value decomposition could also have been used to diagonalise the constant plant TFM. However, such a decomposition would not have the same physical significance as the parameterisation presented in Section 3, where the shape profile is parameterised in terms of the natural bending modes present in the mill [2].

REFERENCES

1. Grimble, M.J. and Fotakis, J. "The design of shape control systems for Sendzimir mills", IEEE Trans. Auto. Con., AC-27, 1982, pp 656-666.
2. Ringwood, J.V., Owens, D.H. and Grimble, M.J. "Feedback design of a canonical multivariable system with application to shape control in Sendzimir mills", submitted Automatica, 1985.
3. Dutton, K. "An investigation into the design and performance of a shape control system for a Sendzimir mill", Ph.D. Thesis, Sheffield City Polytechnic, 1983.
4. Bravington, C.A., Barry, D.C. and McClure, C.H. "Design and development of a shape control system", Proc. Metals Soc. Conf. on Shape Control, Chester, March 1976, pp 82-88.
5. Ringwood, J.V. "The design of shape control systems for a Sendzimir mill", Ph.D. Thesis, University of Strathclyde, 1984.
6. Gunawardene, G.W.D.M. "Static model development for the Sendzimir cold rolling mill", Ph.D. Thesis, Sheffield City Polytechnic, 1982.
7. Beck, J.V. and Arnold, K.J. "Parameter estimation in engineering and science", Wiley.
8. Fisher, R.A. and Yeates, F. "Statistical tables for boilogical, agricultural and medical research", Oliver and Boyd, 1925.
9. Householder, A.S. "Principles of numerical analysis", McGraw-Hill, New York, 1953.
10. Noble, B. "Applied linear algebra", Prentice Hall, New Jersey, 1969.
11. Owens, D.H. and Chotai, A. "Robust control of linear dynamic systems using approximate models", Proc. IEE Part D, 130, 1983, pp 45-57.
12. Lunze, J. "Multidimentional bounds for robust stability studies", Systems and Control Letters, 4, 1984, pp 85-89.
13. Ledermann, W. "Handbook of applicable mathematics Vol.3 - numerical methods", Wiley, 1981.

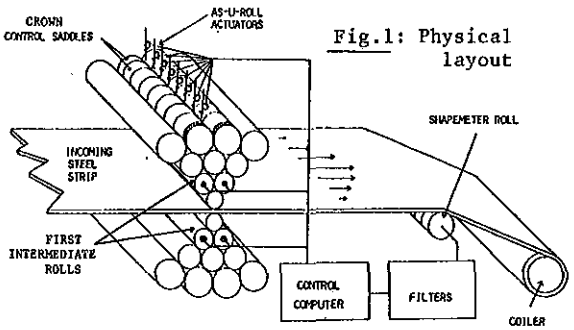

Fig.1: Physical layout

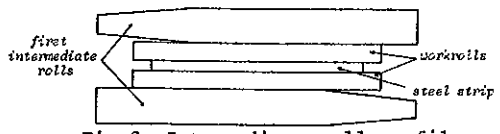

Fig.2: Intermediate roll profile

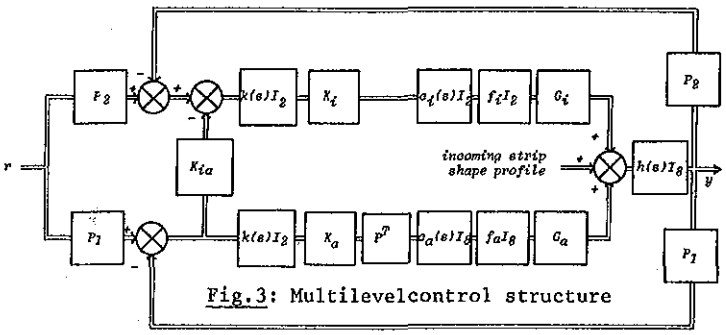

Fig.3: Multilevelcontrol structure

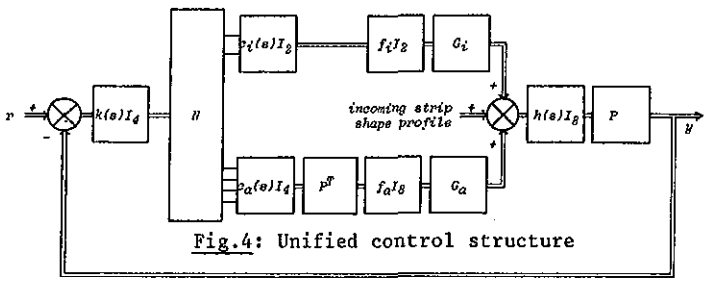

Fig.4: Unified control structure

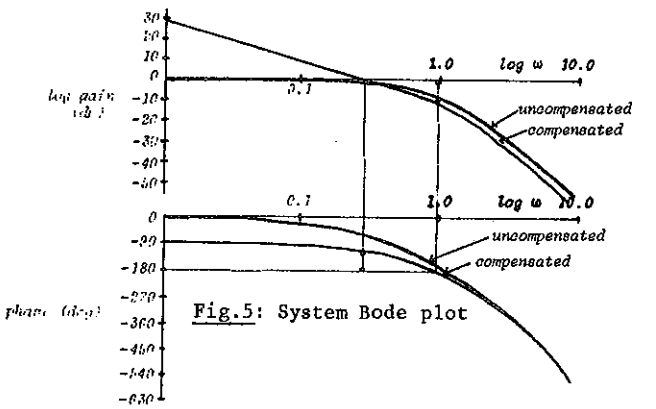

Fig.5: System Bode plot

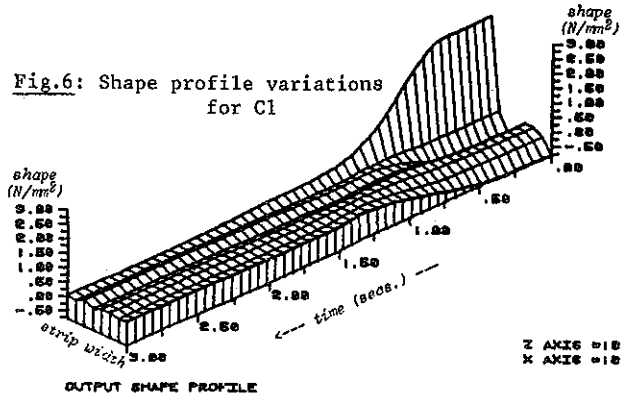

Fig.6: Shape profile variations for C1

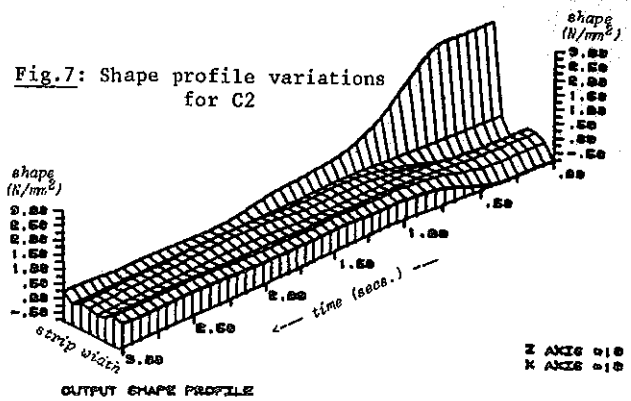

Fig.7: Shape profile variations for C2

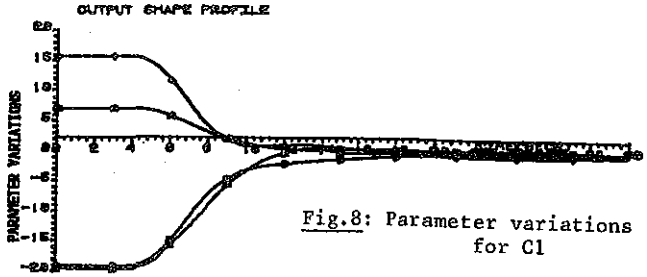

Fig.8: Parameter variations for C1

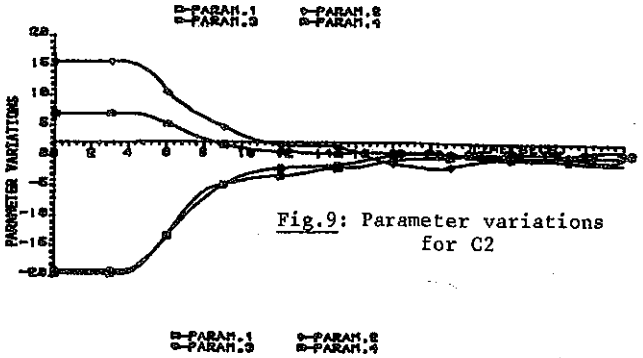

Fig.9: Parameter variations for C2

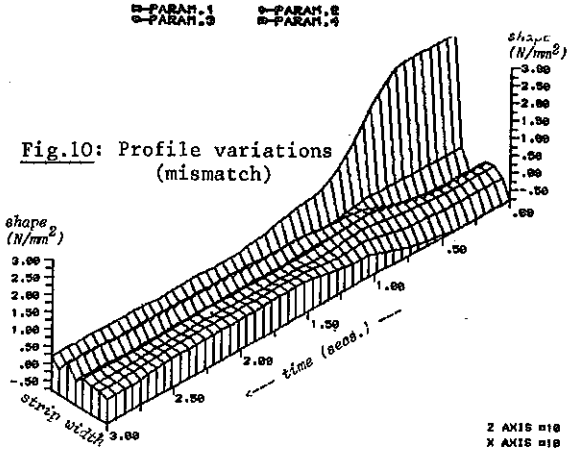

Fig.10: Profile variations (mismatch)

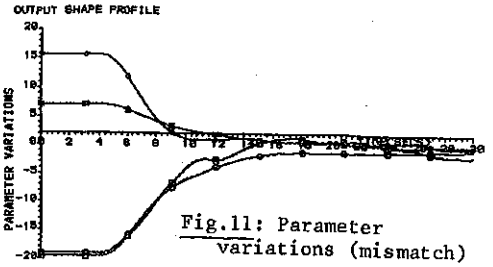

Fig.11: Parameter variations (mismatch)

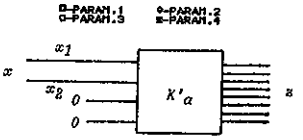

Fig.12